

# Definition of Normal Vertebral Morphometry Using NHANES-II Radiographs

John A. Hipp,<sup>1</sup>  Trevor F. Grieco,<sup>1</sup> Patrick Newman,<sup>1</sup> and Charles A. Reitman<sup>2</sup>

<sup>1</sup>Medical Metrics, Imaging Core Laboratory, Houston, TX, USA

<sup>2</sup>Orthopaedics and Physical Medicine, Medical University of South Carolina, Charleston, SC, USA

## ABSTRACT

A robust definition of normal vertebral morphometry is required to confidently identify abnormalities such as fractures. The Second National Health and Nutrition Examination Survey (NHANES-II) collected a nationwide probability sample to document the health status of the United States. Over 10,000 lateral cervical spine and 7,000 lateral lumbar spine X-rays were collected. Demographic, anthropometric, health, and medical history data were also collected. The coordinates of the vertebral body corners were obtained for each lumbar and cervical vertebra using previously validated, automated technology consisting of a pipeline of neural networks and coded logic. These landmarks were used to calculate six vertebral body morphometry metrics. Descriptive statistics were generated and used to identify and trim outliers from the data. Descriptive statistics were tabulated using the trimmed data for use in quantifying deviation from average for each metric. The dependency of these metrics on sex, age, race, nation of origin, height, weight, and body mass index (BMI) was also assessed. There was low variation in vertebral morphometry after accounting for vertebrae (eg, L1, L2), and the  $R^2$  was high for ANOVAs. Excluding outliers, age, sex, race, nation of origin, height, weight, and BMI were statistically significant for most of the variables, though the F-statistic was very small compared to that for vertebral level. Excluding all variables except vertebra changed the ANOVA  $R^2$  very little. Reference data were generated that could be used to produce standardized metrics in units of SD from mean. This allows for easy identification of abnormalities resulting from vertebral fractures, atypical vertebral body morphometries, and other congenital or degenerative conditions. Standardized metrics also remove the effect of vertebral level, facilitating easy interpretation and enabling data for all vertebrae to be pooled in research studies. © 2022 The Authors. *JBMR Plus* published by Wiley Periodicals LLC on behalf of American Society for Bone and Mineral Research.

**KEY WORDS:** CERVICAL; LUMBAR; NORMAL; VERTEBRAL MORPHOMETRY

## Introduction

Although vertebral fractures can be asymptomatic, such fractures can be a source of symptoms. One of the most important predictors of subsequent fractures is the number of prior fractures.<sup>(1–3)</sup> Vertebral fractures are therefore diagnostically important. Fractures can be difficult to diagnose and are missed in clinical practice.<sup>(4–6)</sup> Ferrar et al. succinctly identified the challenge of fracture detection: “The identification of vertebral fractures is problematic because<sup>(1)</sup> ‘normal’ radiological appearances in the spine vary greatly both among and within individuals<sup>(2)</sup>; ‘normal’ vertebrae may exhibit misleading radiological appearances due to radiographic projection error; and<sup>(3)</sup> ‘abnormal’ appearances due to non-fracture deformities and normal variants are common, but can be difficult to differentiate from true vertebral fracture.”<sup>(7)</sup>

A typical definition of a fracture is “20% or greater loss in expected vertebral body height.” This definition requires

definition of “expected” vertebral body height, and that in turn requires accurate measurements of vertebral body shape in a large and representative population. Validation of the clinically meaningful threshold level for change in vertebral dimensions also requires a reliable reference standard. Inaccuracies in measuring shape and the challenge of finding a suitable reference standard are well documented.<sup>(7–43)</sup> One option is to use the patient’s own adjacent vertebral bodies as a reference, but there is no definitive method for assuring that the adjacent levels are normal or reference data to know how much variability between levels is normal. Normative vertebral body shape metrics that represent a large proportion of the population and account for age, sex, and other confounding factors have not been previously published. Robust reference data and an understanding of the important confounding factors would facilitate more accurate and reproducible diagnosis of the presence and severity of vertebral body fractures.

This is an open access article under the terms of the [Creative Commons Attribution](#) License, which permits use, distribution and reproduction in any medium, provided the original work is properly cited.

Received in original form June 21, 2022; revised form August 8, 2022; accepted August 26, 2022. Accepted manuscript online August 29, 2022.

Address correspondence to: John A. Hipp, PhD, 1632 Summit Lake Shore Rd, NW, Olympia, WA 98502, USA. E-mail: [jhipp@medicalmetrics.com](mailto:jhipp@medicalmetrics.com)

Additional supporting information may be found online in the Supporting Information section.

JBMR<sup>®</sup> Plus (WOA), Vol. 6, No. 10, October 2022, e10677.

DOI: 10.1002/jbm4.10677

© 2022 The Authors. *JBMR Plus* published by Wiley Periodicals LLC on behalf of American Society for Bone and Mineral Research.

Between 1976 and 1980, the Second National Health and Nutrition Examination Survey (NHANES-II) was conducted.<sup>1</sup> This was a nationwide probability sample to document the health status of the United States. Justified by the prevalence and societal impact of neck and back pain, approximately 10,000 lateral cervical spine and 7,000 lateral lumbar spine X-rays were collected as part of this survey. Demographic, anthropometric, health, and medical history data were also collected. This resource can be used for establishing normative reference data that can subsequently be used to diagnose abnormalities such as fractures, vertebral deformities, and congenital abnormalities. These data can also be used to determine whether the sex, age, race, height, weight, or body mass index (BMI) of an individual is needed to predict normal vertebral morphometry.

## Methods

The NHANES-II images and data were obtained through public access.<sup>2</sup> All images were anonymized and identified only by a study ID. A previously validated series of neural networks and coded logic (Spine Camp, Medical Metrics, Inc., Houston, TX) were used to obtain four landmarks for each vertebral body from C2 to C7 and L1 to S1 (Fig. 1). Although the NHANES-II lumbar X-rays almost always included up to T10 in the field of view, the neural networks were only trained to recognize L1 to S1. The cervical spine neural networks were only trained to find C2 to C7. The neural networks include quality control checks to assure the X-ray was a lateral lumbar view and manipulate the image if needed so upper vertebrae are toward the top of the X-ray, with spinous processes toward the left side and with bone being whiter than air. Neural networks and coded logic were then used to segment the bone, find individual vertebrae, label the vertebrae, find the four corners, and finally refrain from reporting landmark coordinates when the confidence of the networks was too low. All the neural networks were trained with over 50,000 lateral X-rays where analysts had previously digitized standardized landmarks. The analysts used Quantitative Motion Analysis software (QMA, Medical Metrics, Inc., Houston, TX) to place the landmarks. The QMA software was previously validated.<sup>(44–49)</sup> NHANES-II images were not used in training the neural networks.

Details of landmark placement are provided in what follows since, as Keynan et al. noted, “There is a lack of standardization in the literature regarding choice and technique for the measurement of these parameters.”<sup>(38)</sup> The standardized landmark placement was focused on the midsagittal plane of each vertebral body (Fig. 1), excluding residual uncinete processes, and placing landmarks that identify the corners of the vertebral bodies prior to any osteophyte formation.<sup>(50, 51)</sup> Landmark placement was similar to that illustrated in Fig. 3 of Genant et al.<sup>(52)</sup> The posterior superior landmarks were placed so as to represent the endplate as it would appear on a midsagittal slice of a CT exam, rather than up at the top of the posterior ridges on the upper endplate, like the logic described in Keynan et al.<sup>(38)</sup> When the X-ray beam path through a vertebra is not perpendicular to the midsagittal plane of the vertebra, the left and right sides of the vertebral endplates or the left and right aspects of the posterior vertebral body may be seen on the X-ray.<sup>(17, 21)</sup> It is understood that radiographic shadows, which might be interpreted as the left and right rims of the endplates, might not exactly represent the endplate rims,<sup>(17)</sup> but it is assumed that the line bisecting these shadows

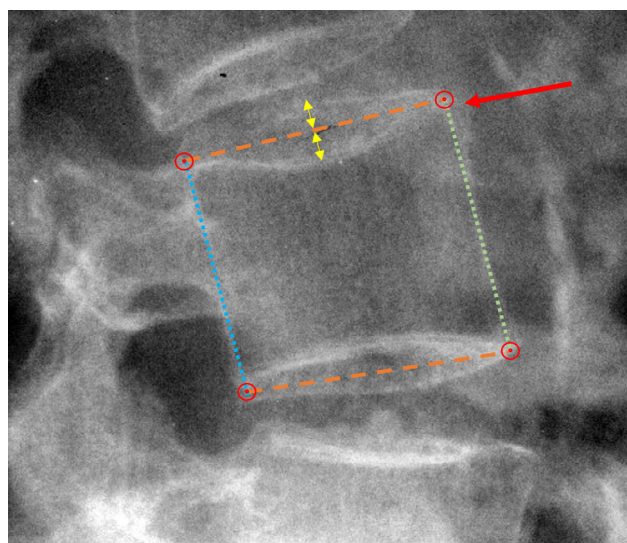


**Fig. 1.** Details of anatomic landmark placement. Dashed lines show assumed midsagittal plane of superior and inferior endplates, identified as bisecting the radiographic shadows of the left and right sides of the endplates (yellow arrows). The red circles show the four landmarks used to measure vertebral body morphometry. The red arrow points to an anterior osteophyte that is ignored. The dotted lines show the anterior and posterior vertebral body heights.

is the best available radiographic approximation of the midsagittal plane. Therefore, the midsagittal plane is assumed to be midway between the radiographic shadows of the left and right sides of endplate and midway between the radiographic shadows of the left and right aspects of the posterior wall. Multiple examples of landmark placement are provided online at <https://www.dropbox.com/sh/qzrocrh86goxarx/AAADRxs5HoEjVdRcGIwA4bela?dl=0>

to help readers appreciate the nuances of how landmarks were placed. Vertebral morphometry calculated from landmarks is dependent on details of landmark placement, and it is therefore important to appreciate landmark placement details. The examples provided include vertebrae with abnormal morphometry (as defined by the metrics presented in this paper). The metrics for each online example are also provided to help readers visualize abnormal morphometry.

The neural networks and coded logic produced landmark coordinates for the vertebral bodies from L1 to S1 in lumbar spine radiographs and C2 to C7 in cervical spine radiographs. An anomaly detection algorithm was then run on those data to identify anomalies due to very poor image quality, severe image artifacts, and very unusual anatomy. Those anomalies were removed from subsequent data analysis.

The coordinates of the four vertebral body corners were used to calculate six vertebral body morphometry metrics that were used in prior studies:

1. anterior/posterior vertebral body height ratio (VBHR),
2. superior/inferior endplate width ratio (EPWR),

<sup>1</sup><https://www.cdc.gov/nchs/nhanes/nhanes2>

<sup>2</sup><https://www.cdc.gov/nchs/nhanes/index.htm>

3. forward/backward diagonal ratio (FBDR),
4. height/width ratio (HWR),
5. angle between superior and inferior endplates (EPA),
6. angle between posterior wall and superior endplate (PSA).

The average of the anterior and posterior heights and the average of the superior and inferior endplate widths were used to calculate the HWR. The metrics are illustrated in Appendix S1: Fig. 1.

The NHANES-II lumbar radiographs were obtained with the subject in the lateral recumbent position with body flexion.<sup>(53)</sup> Because this is not the typical position used to obtain a radiograph for vertebral fracture detection, global and local spinal lordosis were not calculated. The NHANES-II cervical spine radiographs were obtained with the subject standing and a 25-lb weight in each hand to pull down the shoulders and the head and neck flexed forward.<sup>(53)</sup>

Principal component analysis was used to determine whether the dimensionality of the data could be reduced (Stata version 15). The dependency of the six vertebral morphometry metrics on sex, age, race, nation of origin, height, weight, and BMI was assessed using ANOVA (Stata version 15). In the NHANES-II study, race was recorded as white, black, or other. Nation of origin was one of 13 categories.

Descriptive statistics were tabulated and used to identify and trim outliers in the data that might have compromised the definition of “normal” vertebral morphometry.<sup>(54–57)</sup> The data were trimmed by excluding all vertebrae where any of the six metrics was more than 2 SD above or below the mean, and descriptive statistics were tabulated for use in quantifying deviation from average for each metric. Outliers more than 3 SD above or below the mean were inspected to identify typical explanations for each type of outlier. Correlations between the six morphometry metrics were also explored. Finally, means and SDs were tabulated for each metric, for each vertebra from L1 to S1, and from C2 to C7. Those means and SDs were then used to calculate standardized metrics (SDs from mean) for the entire data sets. All statistical analysis was completed using Stata version 15 (College Station, TX, USA).

The NHANES-II study also includes a response to the following question: “Have you ever had pain in your back on most days for at least 2 weeks?” The response to the question was analyzed for associations with the six morphometry metrics. A reproducibility study was also performed and is described in Appendix S2. An assessment of errors that can occur in the morphometry metrics due to variability in radiographic projection is described in Appendix S3.

## Results

### Summary of data analyzed

Computer-generated lumbar landmarks were obtained for 42,980 vertebrae from 7,364 of 7,423 total lumbar radiographs and 54,093 vertebrae from 9,662 out of 9,669 cervical

radiographs for subjects 25–74 years old. Fifty lumbar X-rays were not analyzed due to an error in file transfer, and seven cervical and nine lumbar X-rays were nonanalyzable. Landmark generation for all lumbar and cervical radiographs took 22 hours on a dual computer processing unit (CPU), four graphics processing unit (GPU) (Nvidia T4) production server. The age range was 25–74 years, and the demographic and body size data are summarized in Table 1. The ages of the subjects (using cervical data) were also biased toward older ages (Fig. 2).

Note that females are underrepresented in the lumbar data. By the design of the NHANES-II study, no lumbar X-rays were taken for pregnant women or women under 50.<sup>(58)</sup> An additional limitation relates to the data on race and nation of origin recorded in the NHANES-II data. Based on the cervical data, 86.9% of NHANES-II subjects were “white,” 11.2% were “black,” and the rest were “other.” A more uniform representation of races would likely be needed to fully understand the importance of race. The same is true for the “nation of origin” data in NHANES-II. Note that the text in quotes is as it appears in the NHANES-II documentation: 74.1% of subjects are classified as “OTHER EUROPE SUCH AS GERMAN, FRENCH, ENGLISH, IRISH,” 10.8% as “BLACK, NEGRO OR AFRO-AMERICAN,” and the rest distributed in one of 11 other classifications.

Principal component analysis (PCA) of the lumbar data documented that five primary components explained 99.8% of the variance in the morphometry data, and PCA of the cervical data showed that six components explained 99.7% of the variance. Since PCA does not appreciably reduce the dimensionality of the data, they were not investigated further.

### Descriptive statistics for normative reference

Descriptive statistics for the morphometric parameters are provided in Appendix S1: Tables 1 and 2, after trimming the data. Mean values changed very little for the morphometry metrics after trimming the data, suggesting that normal morphometry is dominant in the data. SDs were reduced after trimming. These observations are the same as reported in a similar study.<sup>(56)</sup> Data with a Gaussian distribution have a skewness of 0 and kurtosis of 3. Trimming the data substantially reduced the skewness from an average of 0.27 to 0.05 and substantially narrowed the tails of the distribution from an average kurtosis of 4.1 to 2.5. This shows that the distribution of data was more Gaussian after trimming. There was remarkably small variation in vertebral morphometry after accounting for vertebrae (eg, L1, L2). The PSA, FBDR, and EPWR generally had the lowest coefficients of variation (Appendix S1: Tables 3 and 4). Figure 3 provides a comparison of VBHR data in Appendix S1: Table 4 with some previously reported morphometry metrics.<sup>(54–57, 59–61)</sup>

### Effect of covariates

ANOVA (after trimming the data) revealed that age, sex, race, and nation of origin were statistically significant for most of the

**Table 1.** Sample size, average age [SD], and average BMI (kg/m<sup>2</sup>) [SD]

Sex	Lumbar			Cervical		
	N	Age	BMI	N	Age	BMI
Male	4,553	50.9 [15.3]	25.5 [4.0]	4,610	50.8 [15.3]	25.5 [4.0]
Female	2,809	63.3 [6.4]	26.4 [5.5]	5,050	51.4 [15.2]	25.8 [5.8]

Age and BMI were missing for two subjects.

Abbreviation: BMI, body mass index.

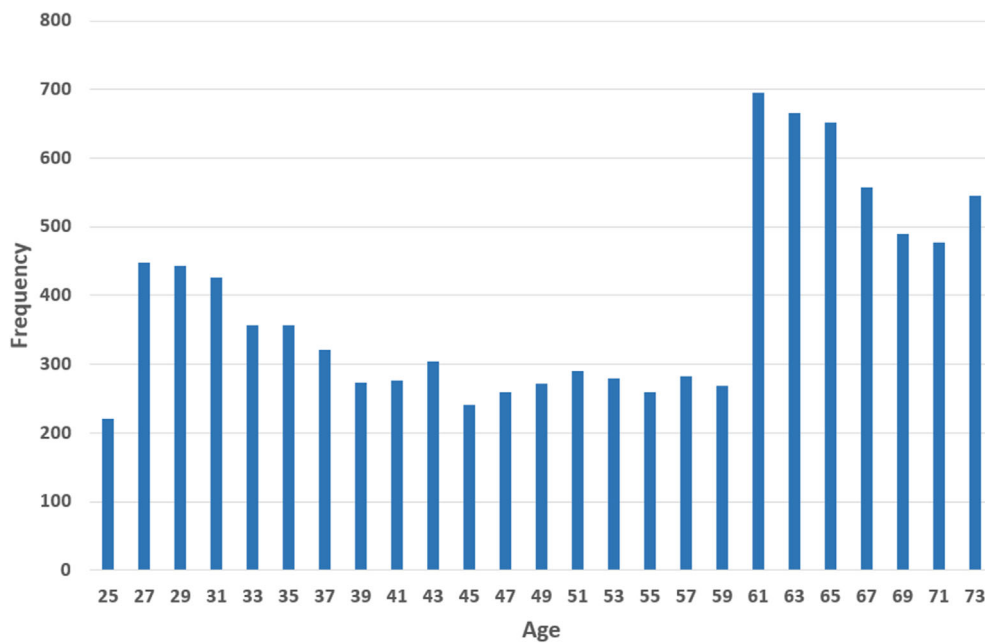


**Fig. 2.** Distribution of ages in Second National Health and Nutrition Examination Survey study.

variables (Appendix S1: Tables 5 and 6), and the  $R^2$  was high for most variables. However, the F-statistic was generally small for all variables except vertebral level. Excluding all variables except vertebral level in the ANOVAs changed the  $R^2$  very little (eg, for the lumbar data, VBHR  $R^2$  went from 0.85 to 0.84 and HWR  $R^2$  went from 0.84 to 0.80). This shows that age, sex, race, and body

size are statistically significant but contribute relatively little to the variability in the morphometry metrics. Therefore, it may be reasonable to pool data across sex, race, and nation of origin, at least for the NHANES-II data.

The six morphometric variables were significantly correlated with each other (Appendix S1: Tables 7 and 8). EPA and VBHR

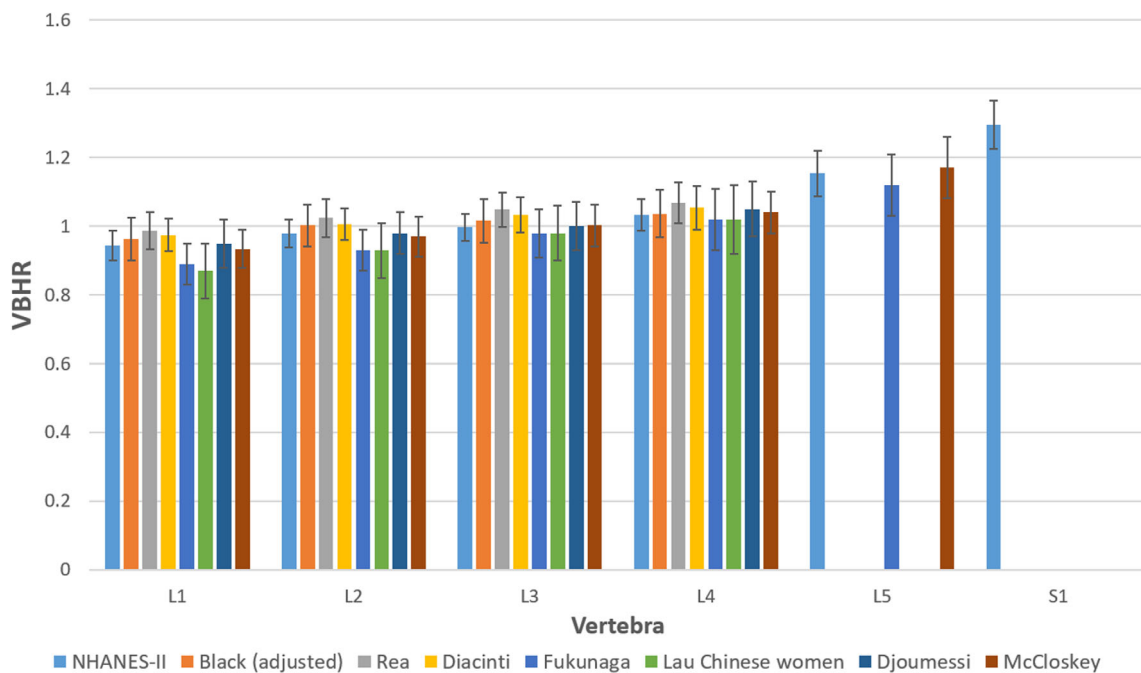


**Fig. 3.** Comparison of previously published vertebral body height ratio data with data obtained from Second National Health and Nutrition Examination Survey.<sup>(54–57, 59–61)</sup>

were almost perfectly correlated, suggesting that only one of these two variables needs to be analyzed. Appendix S1: Tables 9 and 10 provide reference data for the difference between levels in the morphometry metrics.

### Abnormalities in NHANES data

Mean and SD data from Appendix S1: Tables 1 and 2 were used to calculate the vertebra-specific Z-score for each metric according to the following equation:

$$Z = \frac{x - \mu}{\sigma}$$

where  $x$  is the metric for a vertebra,  $\mu$  is the vertebra-specific mean for the corresponding metric, and  $\sigma$  is the vertebra-specific SD for the corresponding metric. Based on these Z-scores, 28,813 of 42,980 lumbar vertebrae (67%) were within  $\pm 2$  SD of average for all six of the metrics. These numbers are less than obtained after trimming since the SDs in Appendix S1: Tables 1 and 2 are smaller than originally used to identify outliers and are therefore more sensitive to abnormalities. Similarly, 36,869 of 54,093 cervical vertebrae (68%) were within  $\pm 2$  SD of average for all six of the metrics.

Box and whisker plots illustrate the magnitude of outliers that exist in the NHANES data (Appendix S1: Figs 2 and 3). Note that the medians are near zero and generally centered within the interquartile range and the whiskers are symmetric. Positive VBHR outliers represent posterior wedge-shaped vertebral bodies, whereas negative VBHR outliers represent anterior wedge-shaped vertebrae. The wedging may be from fractures, remodeling, or congenital conditions, and identifying a specific cause would require more than a single radiograph. Positive EPWR outliers represent vertebrae that are unusually wide superiorly versus inferiorly, and negative outliers are the opposite. Positive and negative FBDR outliers generally appear to be best explained by remodeling, perhaps after a fracture that caused splaying of the fracture fragments. Positive HWR outliers appear as unusually tall vertebrae, whereas negative HWR outliers generally appear to be best explained by a crush fracture. Positive EPA outliers appear as anteriorly wedge-shaped vertebrae, whereas negative outliers appear as posteriorly wedge-shaped vertebrae. Positive PSA outliers generally appear as posterior wedge-shaped vertebrae, and negative outliers generally appear as anteriorly wedge-shaped vertebrae. It is not possible to definitively identify the cause of each abnormality from a single radiograph. Examples of each of high positive and low negative outliers, for each of the six metrics, including landmarks, can be viewed online: <https://www.dropbox.com/sh/qzrocrh86goxarx/AAADRxs5HoEjVdRcGIwA4bela?dl=0>

### Additional observations

Based on logistic regression, the subject response to the question: “Have you ever had pain in your back on most days for at least 2 weeks” was significantly ( $p < 0.05$ ) associated with age, race, and BMI. Since there is no way to determine which vertebra (if any) might be causing back pain, the sum of abnormalities for each subject (metrics  $< -2$  or  $> 2$  SD from the average based on Appendix S1: Table 1) from L1 to S1 was calculated. This sum of abnormalities for the EPWR and the FBDR was significantly associated with the response to the “ever had back pain” question

( $p < 0.05$ ), although the  $R^2$  for these regressions was very small ( $>0.01$ ), indicating a very weak association.

Of the six morphometry metrics, FBDR was the most sensitive and specific metric (area under ROC curve = 0.995) to use for the purpose of using landmarks to classify vertebrae as S1 versus L1–L5. A threshold level of FBDR  $> 1.0574$  misclassified only 278/42,980 vertebrae as S1 versus L1–L5. Including all data for all vertebrae, the proportions of vertebrae with abnormal morphometry ( $<> 2$  SD from average based on Appendix S1: Tables 1 and 2) are summarized in Appendix S1: Tables 11 and 12.

## Discussion

Vertebral morphometry was calculated from landmarks marking the four corners of lumbar and cervical vertebrae. These data may help to establish a reference standard for normal vertebral morphometry that can be used to identify abnormal morphometry, such as can occur as a result of a fracture. The landmarks were produced using a proprietary network of neural networks and coded logic. However, the landmarks are intended to be equivalent to landmarks produced for many prior research studies. Artificial intelligence (AI) has been used to produce vertebral landmarks in many prior studies.<sup>(62–67)</sup> It is expected that the landmark placement obtained for the NHANES-II radiographs can be reproduced by other methods, and the NHANES-II reference data in Appendix S1 will in this way be useful in other studies where landmarks are obtained with alternative methods.

The NHANES-II morphometry data may help in addressing the challenge of accounting for normal variants when assessing for vertebral fractures.<sup>(51, 68)</sup> For example, a somewhat wedge-shaped L5 may be considered a normal variant in clinical practice. Accurate measurements, along with reliable reference data, will help to minimize uncertainty about whether wedging is within normal limits. The question of how much deviation from normal requires clinical intervention remains a challenge. Standardized metrics along with reliable reference data may facilitate the development of computer-aided diagnosis technology.<sup>(69)</sup>

It would have been valuable to obtain data on thoracic vertebral morphometry. The NHANES-II X-rays did capture the whole thoracic spine, and the technology used to obtain landmarks was not trained to place landmarks on thoracic vertebrae, so thoracic vertebral morphometry could not be obtained.

The NHANES-II vertebral morphometry data were based on analysis of lateral spine X-rays. Vertebral morphometry is also assessed from DXA images. The extent to which vertebral morphometry data from X-rays can be applied to DXA scans is poorly understood. This issue has been addressed to an extent,<sup>(70–72)</sup> though no definitive guidance is available. The errors due to variability in radiographic projection described in Appendix S3 are not the same as will occur with DXA scanners, where there would be either no magnification or sagittal plane-only magnification, depending on the scanner. Digitally reconstructed pencil beam, fan beam, and narrow-angle fan beam DXA images could in theory be created from the same CT studies used in Appendix S3 and errors analyzed and compared to X-ray errors. However, that was outside the scope of the study. Diacinti et al. and Rea et al. have published vertebral morphometry data from DXA scanners.<sup>(55, 57)</sup> There are similarities and differences in their reference data for the anterior/posterior vertebral body height ratios for L1 to L4 with VBHR data in Appendix S1. However, further research is needed to determine the applicability of the NHANES-II data to other than lateral spine X-rays.

When the x-ray beam is not coplanar with the endplates and the posterior wall of the vertebra, suboptimal “out-of-plane” images of that vertebra occur. This can occur with suboptimal patient positioning or with scoliosis or lateral listhesis. These out-of-plane images can result in errors in the vertebral morphometry measurements. These errors are explored in Appendices S2 and S3. These errors can be large when the out-of-planeness is pronounced, and caution should be used when interpreting morphometry in these cases.

Considering the correlation between morphometric variables documented in Appendix S1: Tables 7 and 8, VBHR and EPA were almost perfectly correlated, but the other metrics were not. That observation supports the idea that, aside from VBHR and EPA, each of the metrics independently describes some unique aspect of vertebral morphometry. It cannot be determined from the NHANES data alone which of the six metrics will prove most valuable in research and clinical practice. It may be worth exploring the utility of each metric, and combinations of metrics, in future studies where the goal is to diagnose fractures or vertebral deformities.

Multiple prior publications report efforts to establish reference data that can be used to help diagnose vertebral body fractures.<sup>(7–11, 13–16, 18–43)</sup> Although multiple assessments may need to be considered, such as a break or discontinuity in endplates or cortices, intervertebral angles, listhesis, and canal occlusion,<sup>(38, 73)</sup> compression of the vertebral body height is commonly used to help identify fractures. When severe loss of vertebral body height has occurred, clinicians can unanimously agree that a fracture has occurred, but when the fracture is subtle, reference data may be important. Midvertebral landmarks that could be used to measure midvertebral height were not routinely available in the images used to train the neural networks, so midvertebral body heights could not be obtained automatically. Further research is needed to determine the implications of this limitation, although it may be possible to combine morphometric analysis relative to the NHANES reference data with an automated implementation of the Genant classification of fracture morphology.

Change in vertebral shape is considered one of the best indicators of a fracture.<sup>(7)</sup> The NHANES-II images provide only one radiograph per individual, so change in shape could be explored. Nevertheless, the low variability of vertebral shape within a large population supports the potential for using a single X-ray to detect abnormal morphometry with reference to the NHANES-II data. Reporting metrics as SDs from average may also help with interpreting changes in morphometry. It is important to consider the quality and equivalence of radiographic projections when comparing morphometry across time points since variability in radiographic projection can cause potentially misleading apparent changes in morphometry (Appendices S2 and S3). It is also likely that, with advancements in the application of AI to producing spine metrics, the data in Appendix S1: Tables 1 and 2 may provide valuable quality control data to determine whether the AI predictions are aberrant or if caution is warranted in interpreting the results.

Application of the vertebral morphometry metrics, such as in Appendix S1: Tables 1 and 2, to the challenge of documenting vertebral fractures will require defining a threshold level of these metrics that can be used to document the presence/absence of a fracture. Eastell et al. and McCloskey et al. used a threshold of 3 SDs for the VBHR.<sup>(59, 74)</sup> Black et al. used a threshold of 20% difference from normal VBHR.<sup>(26)</sup> Genant et al. used the criterion of a 15% difference compared to the mean VBHR of a normal

population.<sup>(52)</sup> The average VBHR in Appendix S1: Table 1 for L1 to L4 is about 1 and 1 SD is about 0.042, so a 15% difference as used by Genant et al. would be equivalent to approximately a VBHR Z-score of 3.5. A gold-standard test for a vertebral fracture does not exist, so validating a threshold remains a challenge. In addition, L5 may be a special case if the variability in L5 morphometry recognized in the Genant classification confounds the use of a single threshold for all vertebrae. An alternative approach would be to validate a threshold that predicts a positive response to treatment or that predicts subsequent fracture risk. That approach could potentially be retrospectively tested at low cost using automated measurements of morphometry applied to imaging and data from prior studies that collected appropriate imaging. It may also be effective to incorporate a categorical assessment of cortical disruptions or endplate deformations.<sup>(69)</sup> It is likely that these assessments, which are typically made subjectively, can be automated with neural networks given sufficient labeled images for training.<sup>(75, 76)</sup>

It is reasonable to hypothesize that differences in morphometry between adjacent levels may help to identify abnormal morphometry. For example, if one level has an anterior wedge fracture, then a significant difference in the VBHR would be expected when compared to the immediately adjacent levels. A problem occurs when adjacent vertebrae are fractured or otherwise abnormal. Comparison to adjacent levels has been a criterion used or proposed by many investigators, so data that could be used to implement adjacent vertebrae comparisons are provided in Appendix S1: Tables 9 and 10. For example, using data in Appendix S1: Table 9, if the VBHR is to be compared between L4 and L5 vertebrae and normal variability is defined as anything within the 95% confidence interval for data from the NHANES-II study, then the VBHR when comparing L4 to L5 should not vary by more than  $0.124 \pm 1.96 \times 0.059$ , or 0.007 to 0.24.

Some error in the data from Appendix S1: Tables 1 and 2 may occur as a result of the challenges of vertebral labeling. A systematic approach to definitively labeling vertebrae requires whole spine imaging.<sup>(77)</sup> An X-ray or CT of the entire spine from occiput to sacrum was not available, so it cannot be certain that vertebrae were optimally labeled if there were other than five lumbar vertebrae transitional vertebrae or other abnormalities.<sup>(78, 79)</sup> Spines with other than five lumbar vertebrae are uncommon.<sup>(80)</sup> Transitional vertebrae may be more common,<sup>(81)</sup> but it is unclear whether this would consistently compromise labeling from a lateral spine X-ray. The assumption is that the vertebrae were correctly labeled in the majority of data used to train the neural networks and, therefore, were correctly labeled for the majority of the NHANES cases. The possibility of mislabeled vertebrae in a minority of cases should not significantly affect the reference data in Appendix S1: Tables 1 and 2. The prevalence of transitional vertebrae reported in the peer-reviewed literature varies between 4% and 36%.<sup>(82–86)</sup> The prevalence of transitional vertebrae in the NHANES-II radiographs remains undocumented. It is assumed that the error sources discussed previously were random sources of error and would not appreciably affect the means and SDs in Appendix S1: Tables 1 and 2.

One advantage of the six vertebral morphometry metrics is the lack of dependence on radiographic magnification. All metrics are ratios of single vertebral dimensions or angles between anatomic reference lines and should not vary appreciably with radiographic magnification (assuming sufficient spatial resolution). This is important since radiographic magnification can vary substantially between lumbar X-rays,<sup>(87–89)</sup> and this can result in errors in measurements of vertebral dimensions.<sup>(27)</sup>

The NHANES-II data do not uniformly represent all ages, sexes, races, and nations of origin. In particular, it would be valuable to repeat this analysis on X-rays that better represent races and nations of origin not well represented in the NHANES-II data. Djoumessi et al. have reported differences in the VBHR between different nations of origin.<sup>(56)</sup> Other studies showed a dependence of vertebral morphometry on age, gender, race, and other variables, but the relative magnitude of the influence, relative to other covariates, was not described.<sup>(90–94)</sup> That older ages were more common in the NHANES-II data (Fig. 3) may explain the relatively high rate of vertebrae with at least one abnormal morphometry metric.

## Conclusion

The lateral spine lumbar and cervical radiographs from the NHANES-II study were used to establish normative vertebral morphometry reference data. These data can be used to help objectively identify vertebral body fractures, with the assumption that fractures will result in significant deviations from large population-based average vertebral body dimensions. Early diagnosis of fracture allows for early evaluation and prevention, ultimately decreasing deformity as well as risk of future fracture. The data in Appendix S1: Tables 1 and 2 can be used to produce standardized metrics in units of SD from mean. This allows for easy identification of abnormalities resulting from vertebral fractures, atypical vertebral body morphometrics, and other congenital or degenerative conditions and removes the effect of vertebral level, allowing data for all vertebrae to be pooled in research studies. Metrics developed from a large database, such as NHANES-II, should help with differentiating between fractures and normal variants of shape, as this can be challenging.<sup>(95)</sup> This may be one approach to computer-aided diagnosis of vertebral fractures that could supplement classification of vertebral shape, endplate fractures, or use of intra- or intervertebral height ratios.<sup>(96, 97)</sup> Perhaps the greatest challenge is defining the clinically significant fracture that needs to be diagnosed to improve outcomes and lower costs. The deterministic thresholds for standardized metrics that can provide clinically meaningful diagnostic or prognostic information are yet to be determined. These data may also be useful for quality control in technology designed to automatically obtain landmark coordinates and other metrics from medical imaging. This is hopefully a step toward a definitive reference standard that can be universally used in future research. Secondary analysis of existing radiographs may be a promising approach to assessing the efficacy of the reference data.<sup>(98)</sup> With advancements in AI/machine learning, opportunistic analysis of spine X-rays could be near instant and inexpensive and may help to detect undiagnosed fractures if appropriate reference data are used.<sup>(99)</sup>

## Disclosures

John Hipp, Trevor Grieco, and Patrick Newman are employees of Medical Metrics, Inc. No authors have any other relevant conflicts of interest.

## Acknowledgments

No external funding was received in support of this work. The free public access to NHANES-II radiographs is gratefully acknowledged: U.S. Department of Health and Human Services,

Centers for Disease Control and Prevention (CDC), National Center for Health Statistics, National Health and Nutrition Examination Survey Data: [https://www.cdc.gov/nchs/data/nhanes/nhanes\\_release\\_policy.pdf](https://www.cdc.gov/nchs/data/nhanes/nhanes_release_policy.pdf).

## Author Contributions

**Trevor F Grieco:** Data curation; software; writing – review and editing. **Patrick Newman:** Data curation; resources; software. **Charles A Reitman:** Writing – review and editing.

## Ethics Approval

Vertebral morphometry was measured from lateral lumbar and cervical radiographs obtained during the 2nd National Health and Nutrition Survey (1976–1980). That study was designed and conducted to protect the rights of the volunteers, and all subjects in the study signed a consent form, as described in the study documentation: <https://www.cdc.gov/nchs/nhanes/nhanes2/manualsandreports.aspx>; [https://www.cdc.gov/nchs/data/nhanes2/manuals/15a76\\_79.pdf](https://www.cdc.gov/nchs/data/nhanes2/manuals/15a76_79.pdf)

## Peer Review

The peer review history for this article is available at <https://publons.com/publon/10.1002/jbm4.10677>.

## Data Availability Statement

The morphometric data derived from the landmarks are available upon reasonable request.

## References

1. Lindsay R, Silverman SL, Cooper C, et al. Risk of new vertebral fracture in the year following a fracture. *JAMA*. 2001;285(3):320-323.
2. Ross PD, Davis JW, Epstein RS, Wasnich RD. Pre-existing fractures and bone mass predict vertebral fracture incidence in women. *Ann Intern Med*. 1991;114(11):919-923.
3. Lunt M, O'Neill TW, Felsenberg D, et al. Characteristics of a prevalent vertebral deformity predict subsequent vertebral fracture: results from the European prospective osteoporosis study (EPOS). *Bone*. 2003;33(4):505-513.
4. Gehlbach SH, Bigelow C, Heimisdottir M, May S, Walker M, Kirkwood JR. Recognition of vertebral fracture in a clinical setting. *Osteoporos Int*. 2000;11(7):577-582.
5. Delmas PD, van de Langerijt L, Watts NB, et al. Underdiagnosis of vertebral fractures is a worldwide problem: the IMPACT study. *J Bone Miner Res*. 2005;20(4):557-563.
6. Fechtenbaum J, Briot K, Paternotte S, et al. Difficulties in the diagnosis of vertebral fracture in men: agreement between doctors. *Joint Bone Spine*. 2014;81(2):169-174.
7. Ferrar L, Jiang G, Adams J, Eastell R. Identification of vertebral fractures: an update. *Osteoporos Int*. 2005;16(7):717-728.
8. Veleau C, Diaconescu N. Contribution to the clinical anatomy of the vertebral column. Considerations on the stability and the instability at the height of the "vertebral units". *Anat Anz*. 1975;137(3):287-295.
9. Saraste H, Brostrom LA, Aparisi T, Axdorff G. Radiographic measurement of the lumbar spine. A clinical and experimental study in man. *Spine*. 1985;10(3):236-241.
10. Frymoyer JW, Phillips RB, Newberg AH, MacPherson BV. A comparative analysis of the interpretations of lumbar spinal radiographs by chiropractors and medical doctors. *Spine*. 1986;11(10):1020-1023.

11. Gallagher JC, Hedlund LR, Stoner S, Meeger C. Vertebral morphometry: normative data. *Bone Miner*. 1988;4(2):189-196.
12. Davies KM, Recker RR, Heaney RP. Normal vertebral dimensions and normal variation in serial measurements of vertebrae. *J Bone Miner Res*. 1989;4(3):341-349.
13. Smith-Bindman R, Cummings SR, Steiger P, Genant HK. A comparison of morphometric definitions of vertebral fracture. *J Bone Miner Res*. 1991;6(1):25-34.
14. Wang TM, Shih C. Morphometric variations of the lumbar vertebrae between Chinese and Indian adults. *Acta Anat*. 1992;144(1):23-29.
15. Nicholson PH, Haddaway MJ, Davie MW, Evans SF. Vertebral deformity, bone mineral density, back pain and height loss in unscreened women over 50 years. *Osteoporos Int*. 1993;3(6):300-307.
16. O'Neill TW, Varlow J, Felsenberg D, et al. Variation in vertebral height ratios in population studies. European vertebral osteoporosis study group. *J Bone Miner Res*. 1994;9(12):1895-1907.
17. Brinckmann P, Frobin W, Biggemann M, et al. Quantification of overload injuries to thoracolumbar vertebrae and discs in persons exposed to heavy physical exertions or vibration at the work-place: the shape of vertebrae and intervertebral discs—study of a young, healthy population and a middle-aged control group. *Clinical Biomechanics*. 1994;9:S3-S83.
18. Black DM, Palermo L, Nevitt MC, et al. Comparison of methods for defining prevalent vertebral deformities: the study of osteoporotic fractures. *J Bone Miner Res*. 1995;10(6):890-902.
19. Wu CY, Li J, Jergas M, Genant HK. Comparison of semiquantitative and quantitative techniques for the assessment of prevalent and incident vertebral fractures. *Osteoporos Int*. 1995;5(5):354-370.
20. Genant HK, Jergas M, Palermo L, et al. Comparison of semiquantitative visual and quantitative morphometric assessment of prevalent and incident vertebral fractures in osteoporosis the study of osteoporotic fractures research group. *J Bone Miner Res*. 1996;11(7):984-996.
21. Frobin W, Brinckmann P, Biggemann M, Tillotson M, Burton K. Precision measurement of disc height, vertebral height and sagittal plane displacement from lateral radiographic views of the lumbar spine. *Clin Biomech*. 1997;12(Suppl 1):S1-S63.
22. Genant HK. Assessment of vertebral fractures in osteoporosis research. *J Rheumatol*. 1997;24(6):1212-1214.
23. Brinckmann P, Frobin W, Biggemann M, et al. Quantification of overload injuries to thoracolumbar vertebrae and discs in persons exposed to heavy physical exertions or vibration at the workplace part II occurrence and magnitude of overload injury in exposed cohorts. *Clinical Biomechanics*. 1998;13:S1-S36.
24. Espeland A, Korsbrette K, Albrektsen G, Larsen JL. Observer variation in plain radiography of the lumbosacral spine. *Br J Radiol*. 1998;71(844):366-375.
25. Ferrar L, Eastell R. Identification of vertebral deformities in men: comparison of morphometric radiography and morphometric X-ray absorptiometry. *Osteoporos Int*. 1999;10(2):167-174.
26. Black DM, Palermo L, Nevitt MC, et al. Defining incident vertebral deformity: a prospective comparison of several approaches. *J Bone Miner Res*. 1999;14(1):90-101.
27. Weber K, Lunt M, Gowin W, et al. Measurement imprecision in vertebral morphometry of spinal radiographs obtained in the European prospective osteoporosis study: consequences for the identification of prevalent and incident deformities. *Br J Radiol*. 1999;72(862):957-966.
28. Zhou SH, McCarthy ID, McGregor AH, Coombs RR, Hughes SP. Geometrical dimensions of the lower lumbar vertebrae—analysis of data from digitised CT images. *Eur Spine J*. 2000;9(3):242-248.
29. Szulc P, Munoz F, Sornay-Rendu E, et al. Comparison of morphometric assessment of prevalent vertebral deformities in women using different reference data. *Bone*. 2000;27(6):841-846.
30. Ferrar L, Jiang G, Barrington NA, Eastell R. Identification of vertebral deformities in women: comparison of radiological assessment and quantitative morphometry using morphometric radiography and morphometric X-ray absorptiometry. *J Bone Miner Res*. 2000;15(3):575-585.
31. Rea JA, Chen MB, Li J, et al. Morphometric X-ray absorptiometry and morphometric radiography of the spine: a comparison of prevalent vertebral deformity identification. *J Bone Miner Res*. 2000;15(3):564-574.
32. Rea JA, Chen MB, Li J, et al. Vertebral morphometry: a comparison of long-term precision of morphometric X-ray absorptiometry and morphometric radiography in normal and osteoporotic subjects. *Osteoporos Int*. 2001;12(2):158-166.
33. Ferrar L, Jiang G, Eastell R. Vertebral wedge angle measured by morphometric X-ray absorptiometry. *Osteoporos Int*. 2001;12(11):914-921.
34. Szulc P, Munoz F, Marchand F, Delmas PD. Semiquantitative evaluation of prevalent vertebral deformities in men and their relationship with osteoporosis: the MINOS study. *Osteoporos Int*. 2001;12(4):302-310.
35. Frobin W, Leivseth G, Biggemann M, Brinckmann P. Vertebral height, disc height, posteroanterior displacement and dens-atlas gap in the cervical spine: precision measurement protocol and normal data. *Clin Biomech*. 2002;17(6):423-431.
36. Shao Z, Rompe G, Schiltenswolf M. Radiographic changes in the lumbar intervertebral discs and lumbar vertebrae with age. *Spine*. 2002;27(3):263-268.
37. Pfeiffer M, Geisel T. Analysis of a computer-assisted technique for measuring the lumbar spine on radiographs: correlation of two methods. *Acad Radiol*. 2003;10(3):275-282.
38. Keynan O, Fisher CG, Vaccaro A, et al. Radiographic measurement parameters in thoracolumbar fractures: a systematic review and consensus statement of the spine trauma study group. *Spine*. 2006;31(5):E156-E165.
39. Fink HA, Milavetz DL, Palermo L, et al. What proportion of incident radiographic vertebral deformities is clinically diagnosed and vice versa? *J Bone Miner Res*. 2005;20(7):1216-1222.
40. Schwartz EN, Steinberg D. Detection of vertebral fractures. *Curr Osteoporos Rep*. 2005;3(4):126-135.
41. Pflugmacher R, Schroeder RJ, Klostermann CK. Incidence of adjacent vertebral fractures in patients treated with balloon kyphoplasty: two years' prospective follow-up. *Acta Radiol*. 2006;47(8):830-840.
42. Shindle MK, Gardner MJ, Koob J, Bukata S, Cabin JA, Lane JM. Vertebral height restoration in osteoporotic compression fractures: kyphoplasty balloon tamp is superior to postural correction alone. *Osteoporos Int*. 2006;17(12):1815-1819.
43. Siminoski K, Jiang G, Adachi J, et al. Accuracy of height loss during prospective monitoring for detection of incident vertebral fractures. *Osteoporos Int*. 2005;16(4):403-410.
44. Zhao KD, Ben-Abraham EI, Magnuson DJ, et al. Effect of off-axis fluoroscopy imaging on two-dimensional kinematics in the lumbar spine: a dynamic in vitro validation study. *J Biomech Eng*. 2016;138(5):054502.
45. Zhao KD, Yang C, Zhao C, Stans AA, An KN. Assessment of noninvasive intervertebral motion measurements in the lumbar spine. *J Biomechanics*. 2005;38(9):1943-1946.
46. Reitman CA, Hipp JA, Nguyen L, Esses SI. Changes in segmental intervertebral motion adjacent to cervical arthrodesis: a prospective study. *Spine*. 2004;29(11):E221-E226.
47. Reitman CA, Mauro KM, Nguyen L, Ziegler JM, Hipp JA. Intervertebral motion between flexion and extension in asymptomatic individuals. *Spine*. 2004;29(24):2832-2843.
48. Patwardhan AG, Havey RM, Wharton ND, et al. Asymmetric motion distribution between components of a mobile-core lumbar disc prosthesis: an explanation of unequal wear distribution in explanted CHARITE polyethylene cores. *JBJS*. 2012;94(9):846-854.
49. Pearson AM, Spratt KF, Genuario J, et al. Precision of lumbar intervertebral measurements: does a computer-assisted technique improve reliability? *Spine*. 2011;36(7):572-580.
50. Hurxthal LM. Measurement of anterior vertebral compressions and biconcave vertebrae. *Am J Roentgenol Radium Ther Nucl Med*. 1968;103(3):635-644.
51. Diacinti D, Guglielmi G. Vertebral morphometry. *Radiol Clin North Am*. 2010;48(3):561-575.

52. Genant HK, Wu CY, van Kuijk C, Nevitt MC. Vertebral fracture assessment using a semiquantitative technique. *J Bone Miner Res.* 1993;8(9): 1137-1148.
53. CDC. Chapter 13. Examination staff procedures manual for the health and nutrition examination survey, 1976-1979. Hyattsville, MD: National Center for Health Statistics; 1976. pp 2-3. [https://www.cdc.gov/nchs/data/nhanes2/manuals/15a76\\_79.pdf](https://www.cdc.gov/nchs/data/nhanes2/manuals/15a76_79.pdf)
54. Black DM, Cummings SR, Stone K, Hudes E, Palermo L, Steiger P. A new approach to defining normal vertebral dimensions. *J Bone Miner Res.* 1991;6(8):883-892.
55. Diacinti D, Pisani D, Del Fiacco R, et al. Vertebral morphometry by X-ray absorptiometry: which reference data for vertebral heights? *Bone.* 2011;49(3):526-536.
56. Djoumessi RMZ, Maalouf G, Wehbe J, Nehme A, Maalouf N, Seeman E. The varying distribution of intra-and inter-vertebral height ratios determines the prevalence of vertebral fractures. *Bone.* 2004;35(2): 348-356.
57. Rea J, Steiger P, Blake G, Potts E, Smith I, Fogelman I. Morphometric X-ray absorptiometry: reference data for vertebral dimensions. *J Bone Miner Res.* 1998;13(3):464-474.
58. Antani S, Cheng J, Long J, Long LR, Thoma GR. *Medical Validation and CBR of Spine x-Ray Images over the Internet.* Internet Imaging VII: International Society for Optics and Photonics; 2006 p 60610J.
59. McCloskey EV, Spector TD, Eyres KS, et al. The assessment of vertebral deformity: a method for use in population studies and clinical trials [see comments]. *Osteoporos Int.* 1993;3(3):138-147.
60. Fukunaga M, Nakamura T, Shiraki M, et al. Absolute height reduction and percent height ratio of the vertebral body in incident fracture in Japanese women. *J Bone Miner Metab.* 2004;22(2): 104-110.
61. Lau EM, Chan HH, Woo J, et al. Normal ranges for vertebral height ratios and prevalence of vertebral fracture in Hong Kong Chinese: a comparison with American Caucasians. *J Bone Miner Res.* 1996; 11(9):1364-1368.
62. Zhang C, Wang J, He J, Gao P, Xie G. Automated vertebral landmarks and spinal curvature estimation using non-directional part affinity fields. *Neurocomputing.* 2021;438:280-289.
63. Galbusera F, Bassani T, Costa F, Brayda-Bruno M, Zerbi A, Wilke H-J. Artificial neural networks for the recognition of vertebral landmarks in the lumbar spine. *Comput Methods Biomech Biomed Eng.* 2016;6: 1-6.
64. Yeh Y-C, Weng C-H, Huang Y-J, Fu C-J, Tsai T-T, Yeh C-Y. Deep learning approach for automatic landmark detection and alignment analysis in whole-spine lateral radiographs. *Sci Rep.* 2021;11(1):1-15.
65. Zhou S, Yao H, Ma C, et al. Artificial intelligence X-ray measurement technology of anatomical parameters related to lumbosacral stability. *Eur J Radiol.* 2021;146:110071.
66. Cina A, Bassani T, Panico M, et al. 2-step deep learning model for landmarks localization in spine radiographs. *Sci Rep.* 2021;11(1):1-12.
67. Al Arif SMR, Gundry M, Knapp K, Slabaugh G. Improving an Active Shape Model with Random Classification Forest for Segmentation of Cervical Vertebrae. International Workshop on Computational Methods and Clinical Applications for Spine Imaging: Springer; 2016:3-15.
68. Grigoryan M, Guermazi A, Roemer FW, Delmas PD, Genant HK. Recognizing and reporting osteoporotic vertebral fractures. *EurSpine J.* 2003;12(Suppl 2):S104-S112.
69. Lentle B, Koromani F, Brown JP, et al. The radiology of osteoporotic vertebral fractures revisited. *J Bone Miner Res.* 2019;34(3):409-418.
70. Hoyer-Kuhn H, Knoop K, Semler O, et al. Comparison of DXA scans and conventional X-rays for spine morphometry and bone age determination in children. *J Clin Densitom.* 2016;19(2):208-215.
71. Crabtree N, Chapman S, Högl W, et al. Vertebral fractures assessment in children: evaluation of DXA imaging versus conventional spine radiography. *Bone.* 2017;97:168-174.
72. Steiger P, Cummings S, Genant H, Weiss H. Study of osteoporotic fractures research G. morphometric x-ray absorptiometry of the spine: correlation in vivo with morphometric radiography. *Osteo Int.* 1994;4:238-244.
73. Prior J, Oei E, Brown J, Oei L, Koromani F, Lentle BC. Where's the break? Critique of radiographic vertebral fracture diagnostic methods. Springer; 2021:2391-5.
74. Eastell R, Cedel SL, Wahner HW, Riggs BL, Melton LJ 3rd. Classification of vertebral fractures. *J Bone Miner Res.* 1991;6(3):207-215.
75. Derkatch S, Kirby C, Kimelman D, Jozani MJ, Davidson JM, Leslie WD. Identification of vertebral fractures by convolutional neural networks to predict nonvertebral and hip fractures: a registry-based cohort study of dual X-ray absorptiometry. *Radiology.* 2019;293(2):405-411.
76. Monchka BA, Schousboe JT, Davidson MJ, et al. Development of a manufacturer-independent convolutional neural network for the automated identification of vertebral compression fractures in vertebral fracture assessment images using active learning. *Bone.* 2022; 161:116427.
77. O'Brien MF, Kuklo TR, Blanke KM, Lenke LG. *Spinal Deformity Study Group Radiographic Measurement Manual.* Memphis, TN: Medtronic Sofamor Danek; 2005. <https://www.oref.org/docs/default-source/default-document-library/sdsg-radiographic-measurmnt-manual.pdf>.
78. Lian J, Levine N, Cho W. A review of lumbosacral transitional vertebrae and associated vertebral numeration. *Eur Spine J.* 2018;27(5): 995-1004.
79. Shah M, Halalme DR, Sandio A, Tubbs RS, Moisi MD. Anatomical variations that can lead to spine surgery at the wrong level: part III lumbosacral spine. *Cureus.* 2020;12(7):e9433.
80. Abola MV, Teplensky JR, Cooperman DR, Bauer JM, Liu RW. Pelvic incidence in spines with 4 and 6 lumbar vertebrae. *Global Spine J.* 2019; 9(7):708-712.
81. Hanhivaara J, Maatta JH, Niinimäki J, Nevalainen MT. Lumbosacral transitional vertebrae are associated with lumbar degeneration: retrospective evaluation of 3855 consecutive abdominal CT scans. *Eur Radiol.* 2020;30(6):3409-3416.
82. Apazidis A, Ricart PA, Diefenbach CM, Spivak JM. The prevalence of transitional vertebrae in the lumbar spine. *Spine J.* 2011;11(9):858-862.
83. Bron JL, van Royen BJ, Wuisman PI. The clinical significance of lumbosacral transitional anomalies. *Acta Orthop Belg.* 2007;73(6):687-695.
84. Konin GP, Walz DM. Lumbosacral transitional vertebrae: classification, imaging findings, and clinical relevance. *AJNR Am J Neuroradiol.* 2010;31(10):1778-1786.
85. Tang M, Yang XF, Yang SW, et al. Lumbosacral transitional vertebra in a population-based study of 5860 individuals: prevalence and relationship to low back pain. *Eur J Radiol.* 2014;83(9):1679-1682.
86. Nardo L, Alizai H, Virayavanich W, et al. Lumbosacral transitional vertebrae: association with low back pain. *Radiology.* 2012;265(2):497-503.
87. Ravi B, Rampersaud R. Clinical magnification error in lateral spinal digital radiographs. *Spine.* 2008;33(10):E311-E316.
88. Shigematsu H, Koizumi M, Yoneda M, Iida J, Oshima T, Tanaka Y. Magnification error in digital radiographs of the cervical spine against magnetic resonance imaging measurements. *Asian Spine J.* 2013; 7(4):267-272.
89. Lunt M, Gowin W, Johnell AG, Felsenberg D, Study EsgEPO. A statistical method to minimize magnification errors in serial vertebral radiographs. *Osteoporos Int.* 2001;12(11):909-913.
90. Goh S, Tan C, Price RI, et al. Influence of age and gender on thoracic vertebral body shape and disc degeneration: an MR investigation of 169 cases. *J Anat.* 2000;197 Pt 4(4):647-657.
91. Cheng XG, Sun Y, Boonen S, et al. Measurements of vertebral shape by radiographic morphometry: sex differences and relationships with vertebral level and lumbar lordosis. *Skeletal Radiol.* 1998;27(7): 380-384.
92. Sevinc O, Barut C, Is M, Eryoruk N, Safak AA. Influence of age and sex on lumbar vertebral morphometry determined using sagittal magnetic resonance imaging. *Ann Anat Anat Anz.* 2008;190(3):277-283.
93. Ross P, Wasnich R, Davis J, Vogel J. Vertebral dimension differences between Caucasian populations, and between Caucasians and Japanese. *Bone.* 1991;12(2):107-112.
94. Ning L, Song L-J, Fan S-W, et al. Vertebral heights and ratios are not only race-specific, but also gender-and region-specific: establishment of reference values for mainland Chinese. *Arch Osteoporosis.* 2017;12(1):1-9.

95. Diacinti D, Guglielmi G. How to define an osteoporotic vertebral fracture? *Quant Imaging Med Surg*. 2019;9(9):1485.
96. Bromiley PA, Clark EM, Poole KE. Computer-aided diagnostic Systems for Osteoporotic Vertebral Fracture Detection: opportunities and challenges. *J Bone Miner Res*. 2020;35(12):2305.
97. Alqahtani FF, Crabtree NJ, Bromiley PA, et al. Diagnostic performance of morphometric vertebral fracture analysis (MXA) in children using a 33-point software program. *Bone*. 2020;133:115249.
98. Cheng HG, Phillips MR. Secondary analysis of existing data: opportunities and implementation. *Shanghai Arch Psychiatry*. 2014;26(6):371-375.
99. Aggarwal V, Maslen C, Abel RL, et al. Opportunistic diagnosis of osteoporosis, fragile bone strength and vertebral fractures from routine CT scans; a review of approved technology systems and pathways to implementation. *Ther Adv Musculoskelet Dis*. 2021;13:1759720X211024029.